

Planar Array REDOX Cells and pH Sensors for ISS Water Quality and Microbe Detection

Martin G. Buehler, Gregory M. Kuhlman, Nosang V. Myung, and Didier Keymeulen
 Jet Propulsion Laboratory, California Institute of Technology

Samuel P. Kounaves
 Department of Chemistry, Tufts University

Dianne Newman and Douglas Lies
 Department of Geological and Planetary Sciences, California Institute of Technology

Copyright © 2003 SAE International

ABSTRACT

This paper describes results acquired from E-Tongue 2 and E-Tongue 3 which are arrays of planar three-element electrochemical cells and pH sensors. The approach uses ASV (Anodic Stripping Voltammetry) to achieve a detection limit, which in the case of Pb, is below one μM which is needed for water quality measurements. The richness of the detectable species is illustrated with Fe where seven species are identified using the Pourbiac diagram. The detection of multiple species is illustrated using Pb and Cu. The apparatus was used to detect the electroactivity of the metabolic-surrogate, PMS (phenazine-methosulphate). Finally, four types of pH sensors were fabricated and characterized for linearity, sensitivity, and responsiveness.

INTRODUCTION

The goal of this effort is to develop electrochemical sensors that can be used to detect low-levels of electrochemically active species found in drinking water used on the ISS (International Space Station) Alpha and metabolic products produced by biofilms to better understand their life-cycle activities. In pursuing these goals a number of electrochemical cells have been developed. They consist of ISEs (Ion Selective Electrodes) [1], Galvanic cells [2], conductivity sensors [3], REDOX cells [3], and pH sensors. This paper focuses on the development and characterization of REDOX cells and pH sensors.

E-TONGUE 3 APPARATUS

The REDOX sensors found on E-Tongue 3 are shown in Fig. 1. The sensors are fabricated on a 1.25-mm thick 96% alumina substrate. Either Au or Pt-electrodes are screen-printed on the substrates and fired at 900°C in air. As seen in the figure, the substrate consists of nine REDOX cells, a conductivity sensor, a temperature

sensor, and a heater. The substrate is housed in a see-into, flow-through polycarbonate chamber. A water-tight seal is obtained by using O-rings placed on either side of the substrate. The chamber, O-ring, and substrate can be sterilized using an autoclave which exposes these elements to steam at 121°C for 30 minutes.

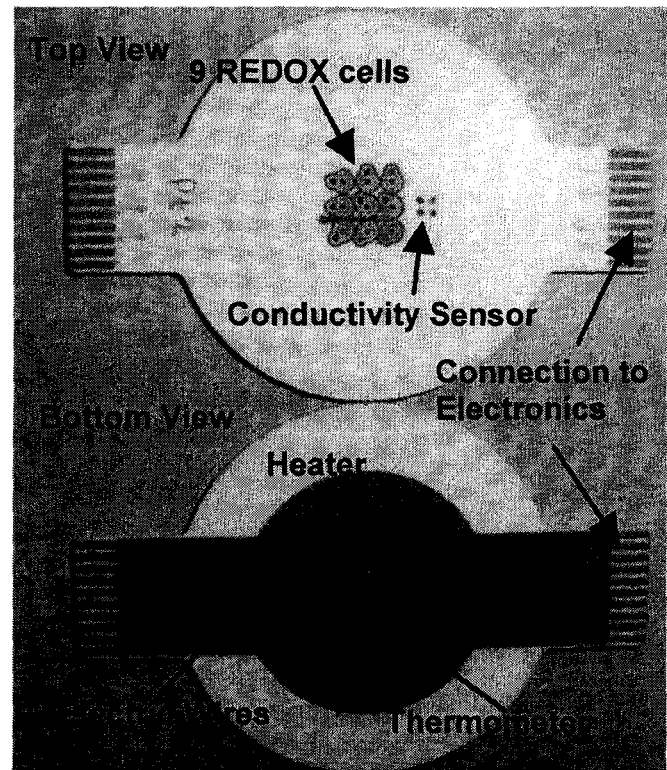


Figure 1. Nine REDOX cells and conductivity sensor are shown in the top view and the heater and thermometer are shown in the bottom view. The long dimension is 6.1 cm.

An overview of the E-Tongue 3 apparatus, shown in Fig. 2, depicts the integration of the ceramic substrate and chamber and electronics board. The chamber contains a 22-mm diameter, 0.15-mm thick cover glass that is

attached to the polycarbonate chamber with RTV rubber. The height of the chamber is 0.5-mm and about 1 mL of solution is required to fill the chamber.

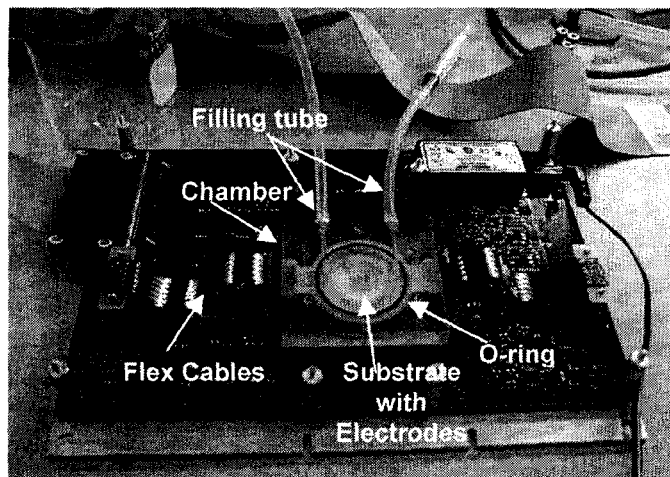


Figure 2. E-Tongue apparatus showing the flex cables that connect the ceramic substrate in the polycarbonate chamber to the electronics on printed wiring board that is 14.3 cm by 21.7 cm.

The apparatus is connected via a ribbon cable seen in the upper-right portion of Fig. 2 to a laptop computer containing a NI-6533 PCMCIA 32-bit digital I/O card. The card is programmed using Visual BASIC to generate the logic needed to control the 11 on-board DACs that generate the wave shapes. Data is acquired from four on-board 12-bit 8-channel ADCs. Each sensor has its own dedicated electronics and so can be individually controlled.



Figure 3. E-Tongue 3 with its top cover attached is placed on the stage of a Zeiss Axioplan microscope.

The REDOX cells and conductivity sensor can be measured in the potentiostat mode, where potential is forced and the current measured, or the galvanostat mode, where current is forced and the voltage measured. Switching between modes is controlled by an electronic switch. In developing E-Tongue 2, it was found

essential to turn off unwanted cells by configuring them in the galvanostat mode with zero current [3]. This prevents unwanted deposition of ionic species onto the electrodes.

In use, the apparatus is placed on a microscope stage as seen in Fig. 3. This application constrained the design because the short vertical movement of the microscope stage. In previous E-Tongue designs [3], access to the sensor electrodes was achieved by a series of pins attached to the underside of the ceramic substrate. Such an approach was unacceptable given the microscope height restrictions. Thus, the substrate was designed to accommodate edge connectors that are attached with flex cables to the electronics. This design approach had the benefit of allowing the substrate to be heat sterilizable since all materials used in its fabrication are fired at a high temperature (900°C). This is important in microbial studies where sterility is a critical issue.

A photomicrograph of the REDOX cell is seen in Fig. 4. In this design the AE electrode completely encloses the cell. As seen in Fig. 1, the AE is electrically common to all other REDOX cells. It is biased at ground potential. This has two benefits: first it reduces the pin count of the array and second, it helps isolate the cells and reduces cell-to-cell cross talk. The WE, working electrode, is biased and its current measured. The apparatus uses a 12-bit ADC with a resolution of 10 nA and current maximum of 50 μ A.

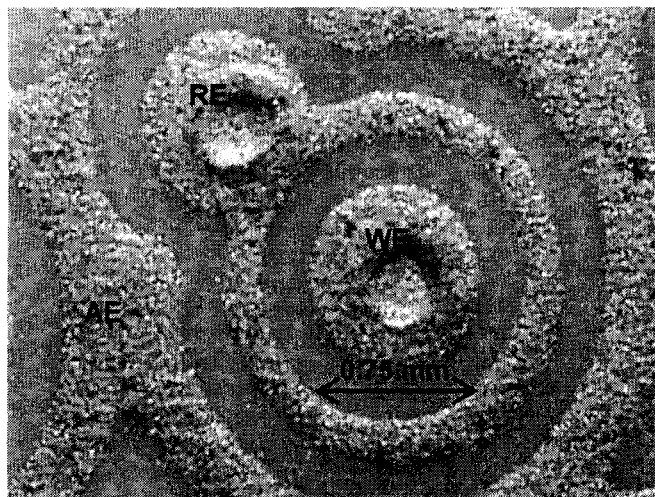


Figure 4. Au REDOX cell with WE (working electrode), RE (reference electrode), and AE (auxiliary electrode). The dimples in the WE and RE are vias used to connect the electrodes to the wires on the bottom of the substrate. The RE ring is 0.125-mm wide and the spacing is 0.25-mm.

The waveform applied to the REDOX cells is shown in Fig 5. First CV (Cyclic Voltammetry) [4] response is measured and then ASV (Anodic Stripping Voltammetry) [5] response is measured after a deposition time, T_{dep} . Both CV and ASV responses are measured twice to validate the repeatability of the measurements. The

magnitude of the waveform slope, S , is identical for both CV and ASV.

Typically $E_1 = +1$ V and $E_2 = -1$ V. These voltages are chosen to stay within the water electrolysis limits where oxygen is generated at the WE for positive potentials and hydrogen at negative potentials. The waveform is applied with T_{dep} values of 10, 20, 50, 100, 200, 500, and 1000s. For this T_{dep} sequence and $S = 20$ mV/s, the measurement takes 132 minutes.

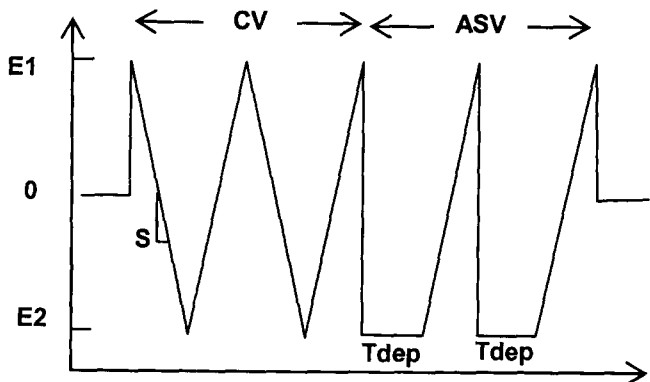


Figure 5. Waveform used to measure the REDOX sensors where S is the slope in mV/s and T_{dep} is the deposition time in s.

EXPERIMENTAL RESULTS

The experimental results are intended to illustrate the breadth of capability of this apparatus. First, the ASV response of $Fe(SO_4)_3$ illustrates how the many species of Fe can be identified using the Pourbiach diagram. Next, the requirements for low-level ion detection is describe with $PbCl_2$ as an example. Next, the capability to detect multiple species is illustrated using $PbCl_2$ and $CuSO_4$. Then the detection of metabolic-compound surrogate, PMS (phenazine-methosulphate) is described. Then, the fabrication of four types of pH sensors are described and characterized for linearity in their response.

The ASV curves included in this report are recent results from E-Tongue 2. Early results from E-Tongue 3 are shown for PMS.

IRON ASV RESPONSE

The CV response for $100 \mu M Fe(SO_4)_3$ is shown in Fig. 6. It indicates that there are numerous electroactive species present. CV curves provide an overview of the species present in solution. In addition they display both reduction (positive to negative scan) and oxidation (negative to positive scan) reactions.

The ASV response, shown in Fig. 7, provides a look at reduction activity and is used to provide quantitative data regarding the species REDOX potential. In Fig. 7 the scan rate is $S = 100$ mV/s and the T_{dep} follows a 1, 2, 5 sequence starting at 10 s and ending at 1000 s.

The identity of the ionic species is determined by matching the experimentally determined REDOX potentials at zero-peak current with known electrochemical potentials. The potential at zero-peak current is determined by extrapolating peak current-voltages to zero current. An Excel software routine, based on analyzing the second derivative [6] of the ASV response, is used to find the peak current-voltages [3].

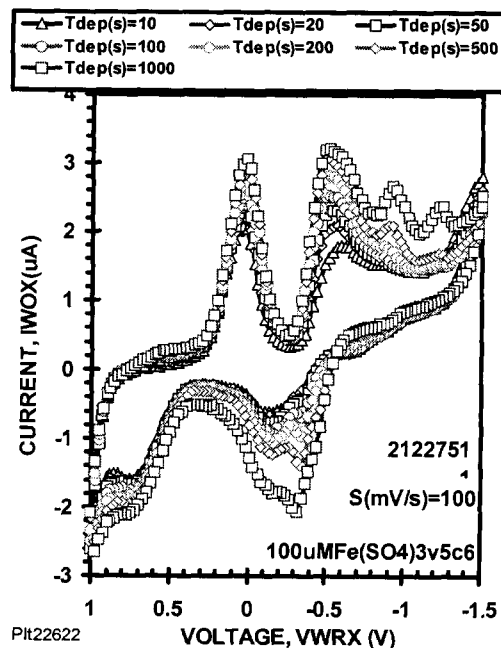


Figure 6. CV response of $100 \mu M Fe(SO_4)_3$ Etg2: WE = Au, RE = Au, AE = Au.

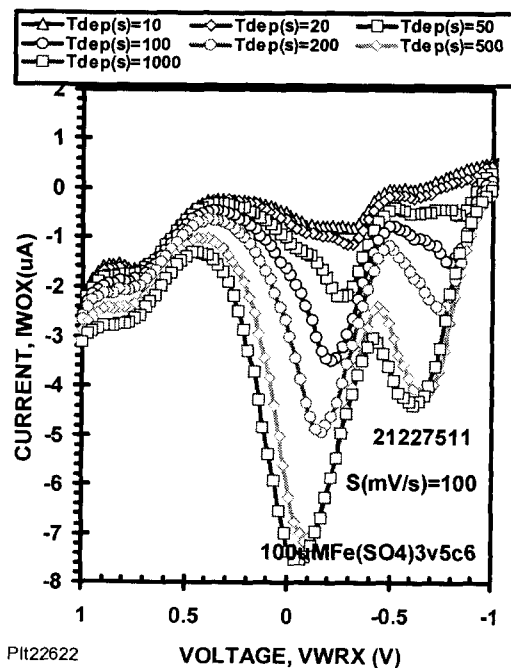


Figure 7. ASV response of $100 \mu M Fe(SO_4)_3$ Etg2: WE = Au, RE = Au, AE = Au.

The analysis of the ASV response for the peak current and voltages is shown in Fig. 8. It reveals that seven reactions are occurring at the WE. The identification of these reactions uses the Pourbaix diagram [7] for iron shown in Fig. 9. During the ASV scan from -1 V to +1 V the Pourbaix is traversed from A to B at pH = 7. The oxidation reactions and their Nernst equations are listed in Table 1.

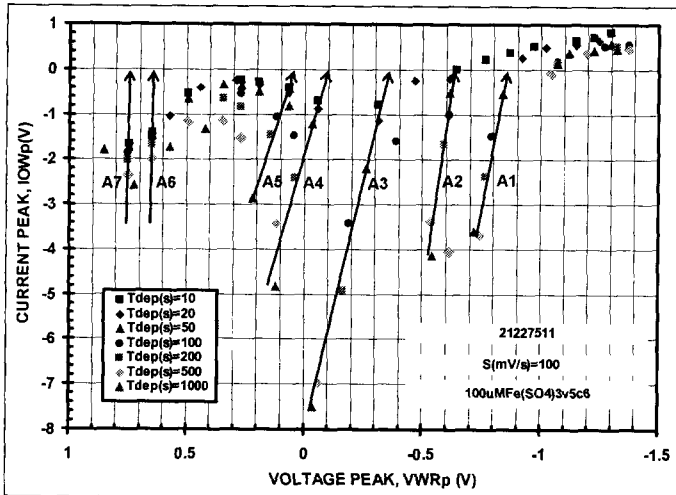


Figure 8. Peak response for 100 μM $\text{Fe}(\text{SO}_4)_3$ derived from Fig. 7.

The reactions listed in Table 1 lead to the following sequence of reactions at the working electrode as the ASV potential is scanned from negative to positive potentials. The first reaction is iron entering solution as Fe^{2+} . Then iron combines with water to form the hydrate, $\text{Fe}(\text{OH})_2$. This hydrate again combines with more water to form the hydrate $\text{Fe}(\text{OH})_3$. Next iron is oxidized to Fe^{3+} . Finally Fe^{2+} in solution near the WE forms Fe^{3+} .

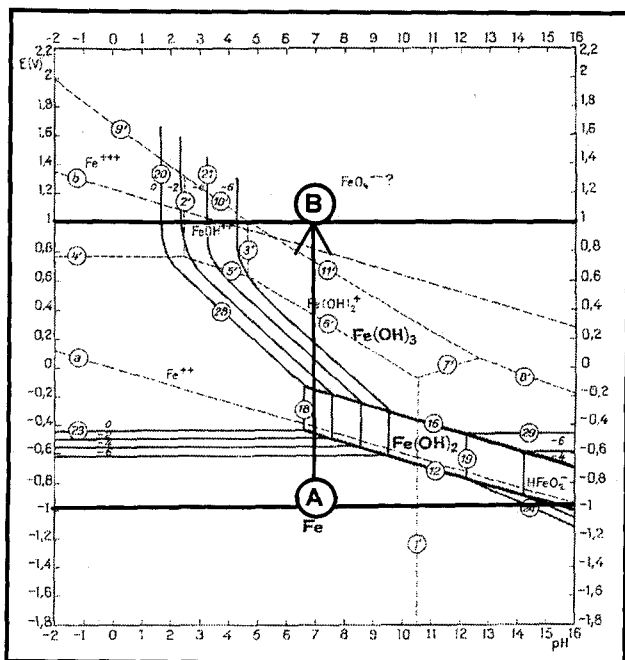


Figure 9. Pourbaix diagram for Iron [7].

Table 1. Iron Reactions for Fig. 8.

NO.	OXIDATION REACTIONS/NERNST EQN.
A1	$\text{Fe} = \text{Fe}^{2+} + 2\text{e}^-$ $E1 = -0.440 + 0.0295 \cdot \log(\text{Fe}^{2+})$
A2	$\text{Fe} + 2\text{H}_2\text{O} = \text{Fe}(\text{OH})_2 + 2\text{H}^+ + 2\text{e}^-$ $E2 = -0.047 - 0.059 \cdot \text{pH}$
A3	$\text{Fe}(\text{OH})_2 + \text{H}_2\text{O} = \text{Fe}(\text{OH})_3 + \text{H}^+ + \text{e}^-$ $E3 = -0.271 - 0.059 \cdot \text{pH}$
A4	$\text{Fe} = \text{Fe}^{3+} + 3\text{e}^-$ $E4 = -0.037 + 0.020 \cdot \log(\text{Fe}^{3+})$
A5	$\text{Fe}^{2+} + 3\text{H}_2\text{O} = \text{Fe}(\text{OH})_3 + \text{H}^+ + \text{e}^-$ $E5 = 1.057 - 0.177 \cdot \text{pH} + 0.059 \cdot \log(\text{Fe}^{2+})$
A6	$\text{Fe}^{2+} = \text{Fe}^{3+} + \text{e}^-$ $E6 = 0.771$
A7	TBD

Peak voltages at zero current derived from Fig. 8 are combined with the potentials derived from the Pourbaix diagram for pH = 7 and concentrations of 100 μM . The result is shown in Fig. 10. The fitting equation is given in the figure. It indicates that the offset voltage is 36 mV and the slope is 1.24. This curve is used to relate the measured peak potentials at zero current to standard electrochemical potentials.

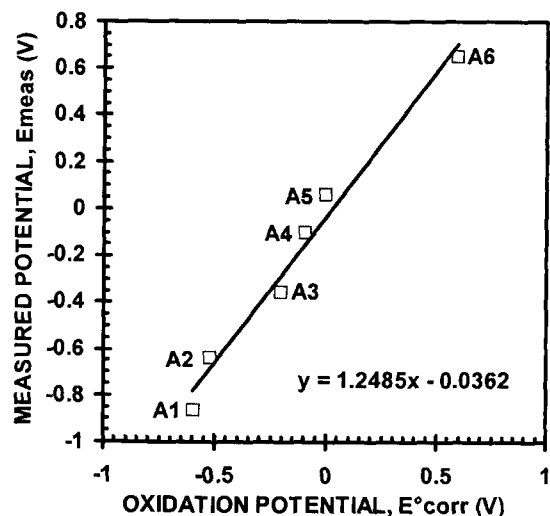


Figure 10. Correlation between measured REDOX potentials derived from Fig. 8 and Pourbaix oxidation potentials derived from Fig. 9.

LOW-LEVEL ASV DETECTION:

Low-level detection of ionic species is important when detecting residual ions in drinking water. The EPA allowable contamination limits for Pb is 0.2 μM . The ASV response of 1- μM of PbCl_2 is shown in Fig. 11. The peak response was achieved by increasing maximum Tdep from 1000 s to 5000 s. As seen in the figure, peaks are clearly visible for Tdeps of 1000, 2000, and 5000 s. This means that low-level detection is possible but requires increased deposition times.

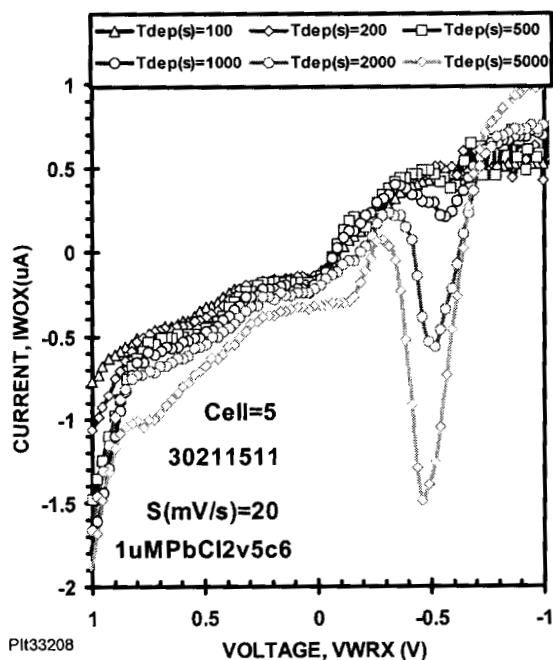


Figure 11. ASV response of 1- μM PbCl_2 . Etg2: WE = RE = AE = Au.

LEAD/COPPER ASV RESPONSE:

In water quality measurements, the ability of ASV to measure multiple contaminants needs to be evaluated. An experiment was devised to determine the effectiveness of ASV to detect Pb and Cu. The oxidation of these cations is separated by about 0.5 V.

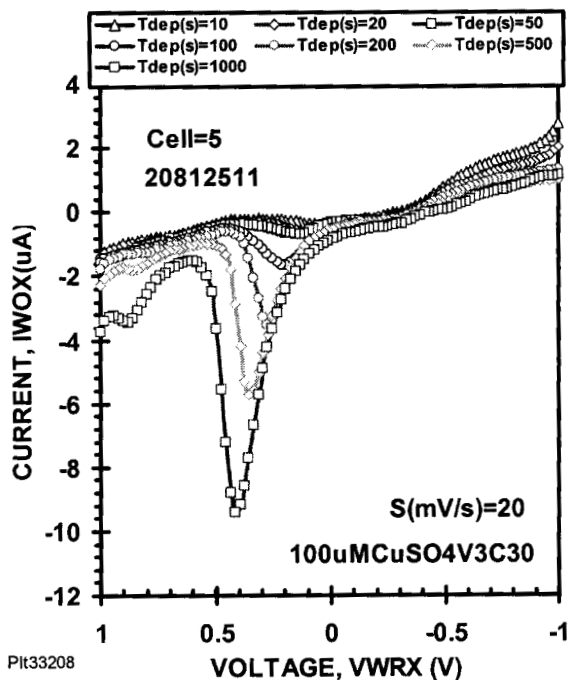


Figure 13. ASV response of 100 μM CuSO_4 . Etg2: WE = Au, RE = Au, AE = Au.

The individual ASV response of Pb and Cu are shown in Figs. 12 and 13, respectively. The combined response is shown in Fig. 14. It is clear that Pb and Cu can be identified. Applying the second derivative analysis to this combined response leads to an identification of the peak potential at zero current as seen in Fig.15.

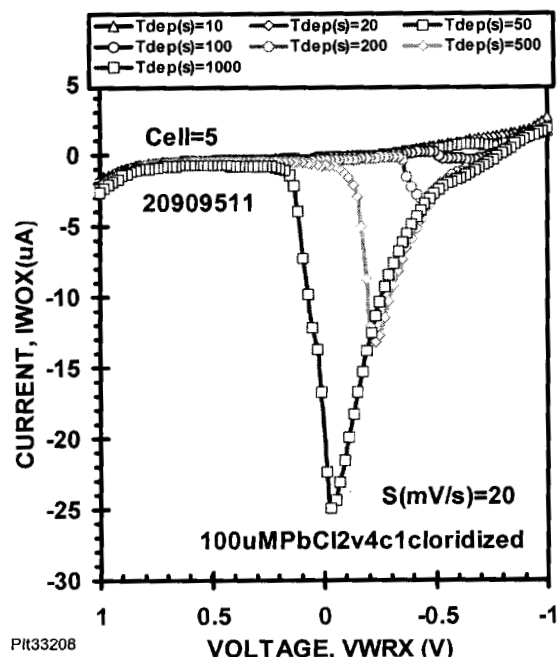


Figure 12. ASV response of 100 μM PbCl_2 . Etg2: WE = Au, RE = AgCl, AE = Au.

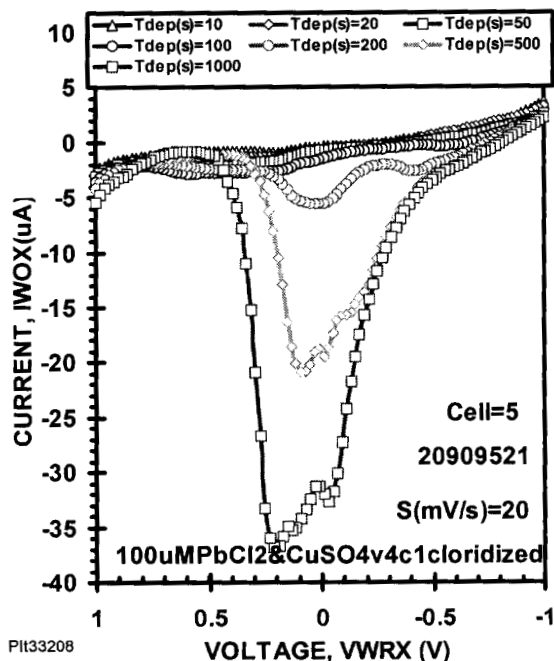


Figure 14. ASV response of 100 μM PbCl_2 and 100 μM CuSO_4 . Etg2: WE = Au, RE = AgCl, AE = Au.

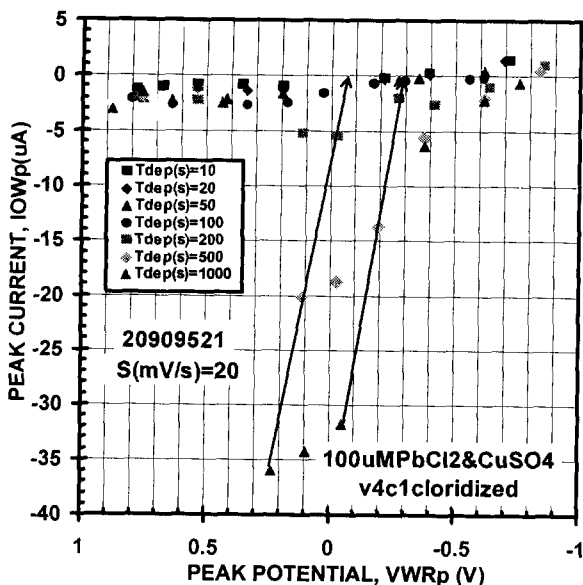


Figure 15. Peak current-voltage response of 100 μM PbCl_2 and 100 μM CuSO_4 . derived from Fig. 14.

MICROBIAL ELECTROACTIVE SPECIES RESPONSE:

E-Tongue 3 was designed to allow simultaneous observation of microbial growth and detection of their electroactive products. PMS (phenazine methosulfate) is a readily available compound that was used to simulate the ASV response of a microbial metabolic product. The response is shown in Fig. 16 and the peak current-voltage analysis is shown in Fig. 17. The analysis shows that two electroactive peaks are present. The peak that appears in the $T_{\text{dep}} = 1000$ s curve in Fig. 16 has not been identified.

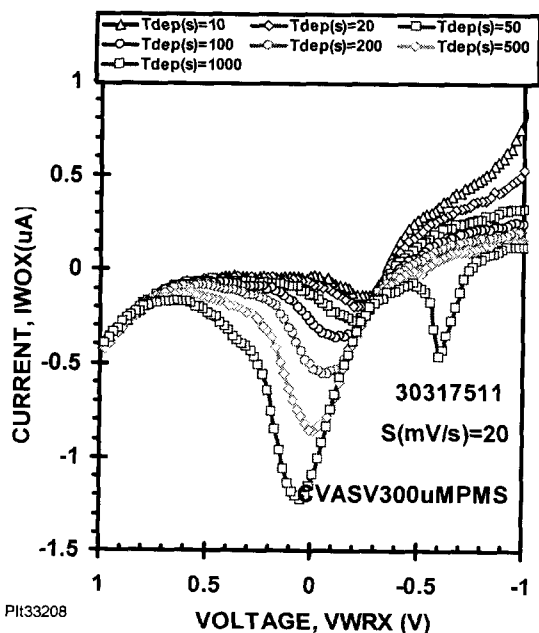


Figure 16. ASV response of 300 μM PMS. Etg3, WE = Au, RE = Au, AE = Au.

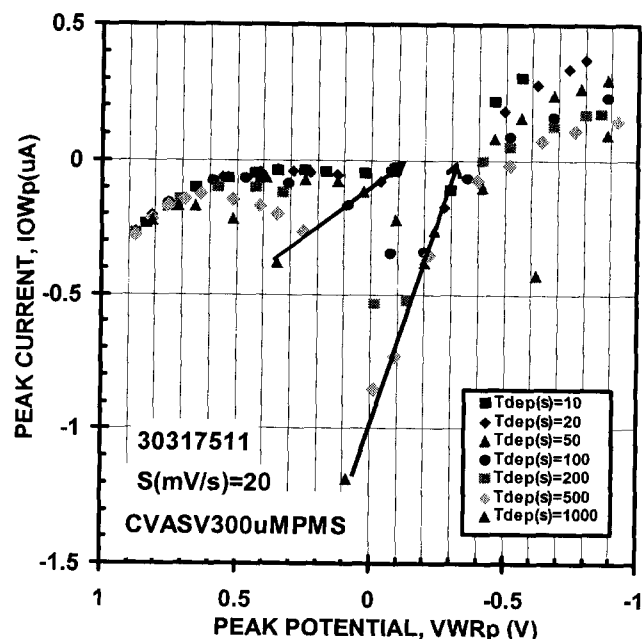


Figure 17 Peak current-voltage response of 300- μM PMS. derived from ASV response in Fig. 20 where $E_1 = -0.32$ V and $E_2 = -0.12$ V.

RESPONSE OF pH SENSORS

Knowledge of pH is critical in identifying electroactive species in solution. This need is supported by the dependence of the REDOX potentials on pH as seen in the Pourbaix diagram in Fig. 9. To fulfill this need, the four pH sensors listed in Table 1 were evaluated. They have fast response time, "drift-free" behavior, show good stability in aggressive environments and are compatible with planar geometries. The pH sensing materials were electrodeposited on gold substrates and integrate into Etongue2.

Table 2. Electrodeposition conditions for various pH sensing materials.

pH Sensor	Electrodeposition Condition
Polyaniline	1 M aniline + 1 M H_2SO_4 , pH < 1, Deposition current density = 4 mA cm^{-2}
Platinum	1 g/l H_2PtCl_6 + 176.4 g/l H_2SO_4 , pH < 1, Deposition current density = -35 mA cm^{-2}
Palladium	10 g/l $\text{Pd}(\text{NH}_2)_2(\text{NO}_2)_2$ + 100 g/l ammonium sulfamate, pH = 7.5 to 8.5, Deposition current density = -1 to -20 mA cm^{-2}
Antimony/Antimony Oxide	20 g/l $\text{K}_2(\text{C}_4\text{H}_4\text{O}_6) \cdot 3\text{H}_2\text{O}$ + 60 g/l $\text{Na}_2\text{C}_4\text{H}_4\text{O}_6 \cdot 2\text{H}_2\text{O}$, pH = 7, Deposition current density = -5 to -20 mA cm^{-2}
Iridium oxide	1.5 g/l H_2IrCl_6 + 5 g/l oxalic acid $[(\text{HCOO})_2 \cdot 2\text{H}_2\text{O}]$ + 1 ml of hydrogen peroxide (H_2O_2), pH = 10.5, Deposition current density < 1 mA cm^{-2}

Figure 18 and Table 3 show the pH response of various electrodeposited sensing materials and their pH sensitivity. Polyaniline (i.e. conducting polymer) and iridium oxide (i.e. metal oxide) show high sensitivity of -85 mV/pH and -76 mV/pH, respectively, with linear response range from pH of 2 to 10. Antimony/antimony oxide electrode shows pH sensitivity of -55 mV/pH with greater detection range from pH of 0 to 12.

Table 3. Sensitivity of pH Sensor

pH Sensing Materials	Sensitivity (mV/pH)
Polyaniline	-85
Platinum	-57
Palladium	-32
Antimony/Antimony Oxide	-55
Iridium oxide	-76

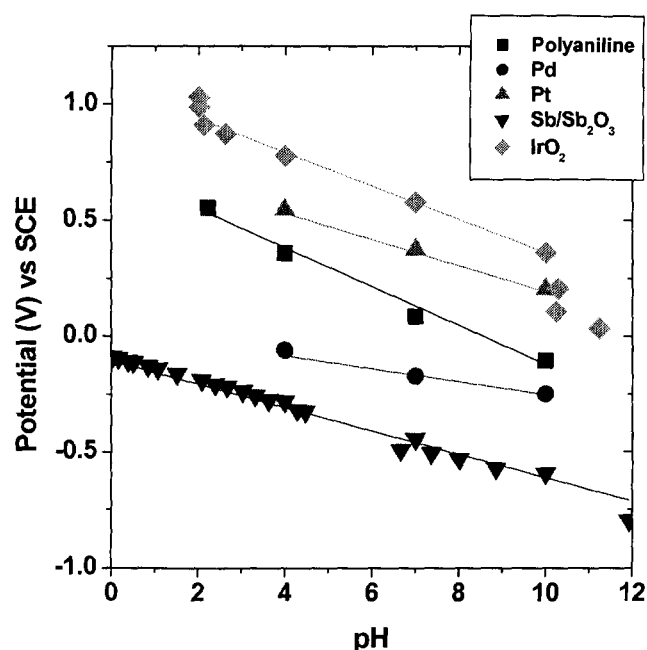


Figure 18. pH responses of various sensing materials: Saturated calomel electrode was used as reference electrode.

Figure 19 shows the dynamic response of polyaniline, platinum, and antimony/antimony oxide electrodes with variation of pH from 10 to 7 using 1 v% H_2SO_4 . Platinum and antimony/antimony oxide electrodes show fast response time (less than few seconds) with good stability. In comparison to platinum and antimony/antimony oxide, the pH response time of polyaniline was slower. This might be due to thicker film thickness of polyaniline (approx. 10 micron) compared to platinum and antimony (< 5 micron). In order to enhance the response time, the optimization of film thickness is in progress.

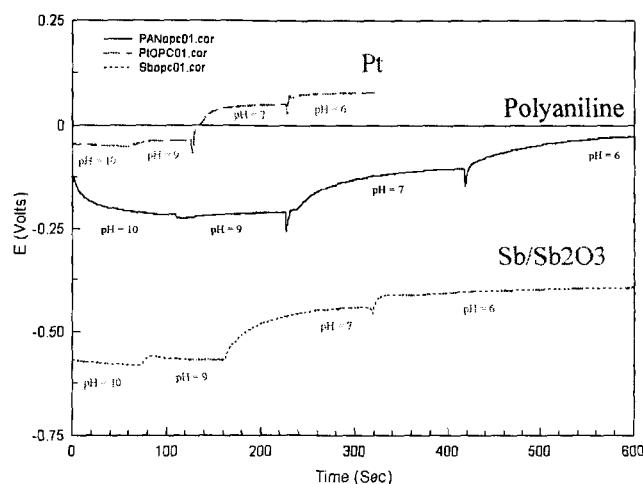


Figure 19. Dynamic pH response of Pt, Polyaniline, and Sb/Sb_2O_3 electrodes. Electrodeposited $Ag/AgCl$ was used as reference electrodes.

CONCLUSION

The E-Tongue sensor has the ability to detect a number of species in solution. In the case of Fe, six species were identified. In water quality measurements it is necessary to be able to identify more than one contaminant simultaneously. A mixture of $PbCl_2$ and $CuSO_4$ was characterized and the mixture response was significantly different from the individual responses. That is, the mixture showed double peaking; whereas, the individual responses did not. Low-level detection is also important for water quality. The detection limit for $PbCl_2$ was shown to be less than $1 \mu M$ requiring deposition time between 1000 and 5000 s. The apparatus was also used to detect the organics, PMS. This compound is a metabolic product stimulant and its detection is important for both water quality and for future biofilm studies. Finally, four pH sensors were fabricated and characterized. They have good sensitivity and stability and will provide additional data needed to identify ionic species using Pourbaix diagrams.

ACKNOWLEDGMENTS

The work described in this paper was performed by the Jet Propulsion Laboratory, California Institute of Technology, under a contract with the National Aeronautics and Space Administration and the Defense Advanced Research Projects Agency. The effort is supported by a grant from the National Aeronautics and Space Administration under the Advanced Environmental Monitoring and Control Program and by the Defense Advanced Research Projects Agency under the Single Layered and Imbedded Microbial Environments Program supporting a contract entitled *Microbial detection using Biofilm Signal Amplification* (Contract: N66001-02-C-8049). The authors are indebted to the NASA program manager, Darrell Jan, for his support. In addition, we are pleased to acknowledge the efforts of Dennis Martin and Kent Fung, Halcyon

Microelectronics, Inc. Irwindale, CA in the fabrication of E-Tongue 3. File: ICES-REDOX3322.doc.

REFERENCES

1. Samuel P. Kounaves, Stefan R. Lukow, Brian P. Comeau, Michael H. Hecht, Sabrina M. Grannan-Feldman, Ken Manatt, Steven J. West, Xiaowen Wen, Martin Frant, and Tim Gillette, "The MSP01 MECA Wet Chemistry Lab: Sensor Evaluation", *Journal of Geophysical Research (Planets)* September 2002
2. Mark Kolody,
3. Martin G. Buehler, Gregory M. Kuhlman, Didier Keymeulen, and Nosang V. Myung, and Samuel P. Kounaves, "Planar REDOX and Conductivity Sensors for ISS Water Quality Measurements" *2003 IEEE Aerospace Conference*, 2003, Vol. 1, cat. No. 02TH8593C.
4. A. J. Bard and L. R. Faulkner, *Electrochemical Methods*, 2nd Edition, Wiley & Sons (New York, 2001).
5. J. Wang, *Analytical Electrochemistry*, Wiley-VCH, New York, 2000.

6. D. Diamond and V. C. A. Hanratty, *Spreadsheet Applications in Chemistry using Microsoft Excel*, J. Wiley & Sons (New York, 1997).

7. M. Pourbaix, "Atlas of Electrochemical Equilibria in Aqueous Solutions", Nation Association of Corrosion Engineers (Houston, TX 1974).

CONTACT

Martin G. Buehler received the BSEE and MSEE from Duke University in 1961 and 1963, respectively and the Ph.D. in EE from Stanford University in 1966 specializing in Solid State Electronics. He worked at Texas Instruments for six years, at National Bureau of Standards (now NIST) for eight years, and since 1981 has been at the Jet Propulsion Laboratory where he is a senior research scientist. At JPL he has developed p-FET radiation monitors for CRRES, Clementine, TELSTAR and STRV, E-nose which flew on STS-95, and an electrometer for the Mars '01 robot arm. In 2002 he received a Snoopy for his contribution to the E-Nose. Starting in September 2002, he spent six months on leave from JPL to studying biofilms and their effect on electrochemical sensors at Caltech in the Geological and Planetary Sciences Department. Martin is a member of the IEEE, Tau Beta Pi, and Sigma Nu. He holds 12 patents and has published over one hundred papers. His e-mail is martin.g.buehler@jpl.nasa.gov.